Technical report from Automatic Control at Linköpings universitet

Unifying the Parity-Space and GLR Approach to Fault Detection with an IMU Application

David Törnqvist, Fredrik Gustafsson

Division of Automatic Control

E-mail: tornqvist@isy.liu.se, fredrik@isy.liu.se

3rd October 2008

Report no.: LiTH-ISY-R-2862
Submitted to Automatica

Address:
Department of Electrical Engineering
Linköpings universitet
SE-581 83 Linköping, Sweden

WWW: http://www.control.isy.liu.se

AUTOMATIC CONTROL
REGLERTEKNIK
LINKÖPINGS UNIVERSITET

Abstract

Using the parity-space approach, a residual is formed by applying a projection to a batch of observed data and this is a well established approach to fault detection. Based on a stochastic state space model, the parity-space residual can be put into a stochastic framework where conventional hypothesis tests apply. In an on-line application, the batch of data corresponds to a sliding window and in this contribution we develop an improved on-line algorithm that extends the parity-space approach by taking prior information from previous observations into account. For detection of faults, the Generalized Likelihood Ratio (GLR) test is used. This framework allows for including prior information about the initial state, yielding a test statistic with a significantly higher sensitivity to faults. Another key advantage with this approach is that it can be extended to nonlinear systems using an arbitrary nonlinear filter for state estimation, and a linearized model around a nominal state trajectory in the sliding window. We demonstrate the algorithm on data from an Inertial Measurement Unit (IMU), where small and incipient magnetic disturbances are detected using a nonlinear system model.

Keywords: fault detection, parity space sensor fusion, inertial sensors, magnetometer.

Unifying the Parity-Space and GLR Approach to Fault Detection with an IMU Application

David Törnqvist and Fredrik Gustafsson

Linköping University
Division of Automatic Control
Department of Electrical Engineering
SE-581 83 Linköping, Sweden

Abstract

Using the parity-space approach, a residual is formed by applying a projection to a batch of observed data and this is a well established approach to fault detection. Based on a stochastic state space model, the parity-space residual can be put into a stochastic framework where conventional hypothesis tests apply. In an on-line application, the batch of data corresponds to a sliding window and in this contribution we develop an improved on-line algorithm that extends the parity-space approach by taking prior information from previous observations into account. For detection of faults, the Generalized Likelihood Ratio (GLR) test is used. This framework allows for including prior information about the initial state, yielding a test statistic with a significantly higher sensitivity to faults. Another key advantage with this approach is that it can be extended to nonlinear systems using an arbitrary nonlinear filter for state estimation, and a linearized model around a nominal state trajectory in the sliding window. We demonstrate the algorithm on data from an Inertial Measurement Unit (IMU), where small and incipient magnetic disturbances are detected using a nonlinear system model.

1 Introduction

The parity-space method is a widely used method to find a residual for fault detection. It was first described in [4], but is described and used in many publications for example [2, 5, 7, 8]. The parity-space approach is a well established approach to fault detection, and one of its main features is the intuitive geometrical interpretation of the residual that is obtained by projecting a batch of observations onto the parity space. The projection assures that the influence of the unknown initial state in the data batch as well as external disturbances do not affect the residual from which diagnosis decisions are made.

The classical parity-space approach applies to linear deterministic models, and has been extended to a statistical framework [11, 12, 6], which makes it applicable to stochastic linear state-space models with additive faults. The performance limits for various noise distributions have been studied in [13]. Its main limitations are:

- It may have a poor sensitivity to faults, in particular for short data batches.
- It cannot handle prior knowledge about the initial state. For instance, a state estimate may be available from observations outside the sliding window.
- It is not easily extended to nonlinear systems.

It is the purpose of this contribution to extend the stochastic parity-space approach to handle these drawbacks.

The main idea is to incorporate prior information of the state when forming the residual. In this way, the sensitivity to faults increases automatically. This increased sensitivity can be used to keep the batch window short while keeping a sufficient sensitivity to faults and in this way decrease the delay until detection. The final result is an algorithm which is related to one of the methods suggested in [19]. This seminal paper applies the Generalized Likelihood Ratio (GLR) test to the same stochastic state-space model, and to limit the computational complexity, the authors propose an algorithm where faults are restricted to a sliding time window. The final algorithm consists of two filters from which all relevant test statistics can be computed.

Further, with a good prior of the initial state and a short batch window, nonlinear systems can be linearized along a nominal trajectory and the parity-space residual is ap-

Email addresses: tornqvist@isy.liu.se (David Törnqvist), fredrik@isy.liu.se (Fredrik Gustafsson).

proximated using the linearized model. The shorter window, the better approximation. This means that a nonlinear filter, as the Extended Kalman Filter (EKF), the Unscented Kalman Filter (UKF) or the Particle Filter (PF), can be run on-line with a time lag corresponding to the batch window, and the residual is continuously monitored on this batch window. If a fault is detected, the filter can be put in simulation mode. The ability to handle nonlinear models in a natural way is a clear improvement to the GLR test in [19].

To demonstrate the algorithm, an application of estimating orientation based on measurements from an Inertial Measurement Unit (IMU) is studied. The unit consists of accelerometers, gyroscopes and magnetometers. This is a classical filtering problem, where the state-space model basically says that the orientation is the integral of measured gyroscope values. This model is subject to a drift which evolves linearly in time, and needs external support. Here, the magnetic field sensors normally functions as a compass and provides a measurement with two degrees of freedom, and the accelerometer can, if there is no external acceleration, be used as an inclinometer providing a measurement relation with three degrees of freedom.

The outline is as follows. Section 2 defines the models used. Using these models, various ways of estimating the initial state in a time window is described in Section 3. The parity-space approach and its relation to different initial state estimates is then described in Section 4. Using the parity-space residuals formed in Section 4, the GLR test in Section 5 can be used for detection. The framework is applied to detect magnetic disturbances in Section 6. Finally, conclusions are provided in Section 7.

2 Modeling

This section describes the relation between state-space modeling and modeling over a sliding window or batch. An efficient fault parameterization is also introduced.

2.1 System Model

Let us consider a discrete-time dynamical system in the form

$$x_{t+1} = F_t x_t + G_t^u u_t + G_t^f f_t + G_t^v v_t, \tag{1a}$$

$$y_t = H_t x_t + H_t^u u_t + H_t^f f_t + e_t, \tag{1b}$$

where x_t is the state vector, u_t an input signal, f_t a scalar time-varying fault profile, y_t a measurement, v_t process noise and e_t the measurement noise. The fault detection test can here be stated as testing if $f_t = 0$ or $f_t \neq 0$.

2.2 Batch Model

The batch form is often used in fault detection and diagnosis [4, 8, 10]. Stack L signal values to define the batched signal vectors like $\mathbb{Y} = \left(y_{t-L+1}^T, \ldots, y_t^T\right)^T$, for all signals. Then, the outputs in that window will be given by

$$\mathbb{Y} = \mathcal{O}_t x_{t-L+1} + \bar{H}_t^u \mathbb{U} + \bar{H}_t^f \mathbb{F} + \bar{H}_t^v \mathbb{V} + \mathbb{E}, \tag{2}$$

with the extended observability matrix

$$\mathcal{O}_t = \begin{pmatrix} H_{t-L+1} \\ H_{t-L+2} F_{t-L+1} \\ \vdots \\ H_t \prod_{k=t-1}^{t-L+1} F_k \end{pmatrix}. \tag{3}$$

The matrices determining how the remaining signals affect the system are described by

$$\bar{H}_t^s = \begin{pmatrix} H_{t-L+1}^s & 0 & \cdots & 0 \\ H_{t-L+2} G_{t-L+1}^s & H_{t-L+2}^s & \cdots & 0 \\ \vdots & & \ddots & \vdots \\ H_t \prod_{k=t-1}^{t-L+2} F_k G_{t-L+1}^s & \cdots & H_t G_{t-1}^s & H_t^s \end{pmatrix}, \tag{4}$$

where $s = \{u, f, v\}$. For simplicity, denote $\mathbb{Z} = \mathbb{Y} - \bar{H}_t^u \mathbb{U}$, implying that the system (2) can be written as

$$\mathbb{Z} = \mathcal{O}_t x_{t-L+1} + \bar{H}_t^f \mathbb{F} + \bar{H}_t^v \mathbb{V} + \mathbb{E}. \tag{5}$$

The system is assumed to be observable, that is, $\mathcal{O}_t$ has full column rank and all states will have a unique influence in the output. However, it is often possible to observe a subspace of the state space and the system can therefore be partially observable. In order to handle such a system, the observable subspace has to be determined. It is given by the singular value decomposition

$$\mathcal{O}_t = U_1 \Sigma V_1^T, \tag{6}$$

where U_1 spans the observable subspace. The state $\bar{x} \triangleq \Sigma V_1^T x$ ($\dim(\bar{x}) < \dim(x)$) is now an observable state. The system (2) can then be rewritten as

$$\mathbb{Y} = U_1 \bar{x} + \bar{H}_t^u \mathbb{U} + \bar{H}_t^f \mathbb{F} + \bar{H}_t^v \mathbb{V} + \mathbb{E}. \tag{7}$$

Now, all methods described in this article can be used with $\mathcal{O}_t$ exchanged for U_1. When a prior estimate of the original estimate is available, as in Section 3.4, the state

estimate and its covariance have to be transformed as

$$\hat{\tilde{x}}^{(1)} = \Sigma V_1^T \hat{x}^{(1)} \tag{8}$$

$$P^{(1)}_{\hat{\tilde{x}}^{(1)}} = \Sigma V_1^T P^{(1)} V_1 \Sigma. \tag{9}$$

2.3 Fault Model

It is convenient for the analysis to assume that the fault is constant over time, while in practice a fault is often increasing or decreasing slowly in magnitude over time. To include such incipient faults, the fault profile f_t can be modeled with a low dimensional parametrization as

$$\mathbb{F} = \Phi^T \theta_t \Rightarrow \bar{H}^\theta \triangleq \bar{H}^f \Phi^T. \tag{10}$$

For the batch model, this model implies that the fault parameter can be considered constant over the data window. Thus, a scalar time-varying parameter is replaced with a constant vector. This facilitates the analysis significantly.

In this paper, the Chebyshev polynomial is used as basis functions, see [1, 17]. An example of the first three basis functions which are orthogonal Chebyshev polynomials over a window of 10 samples is given in Figure 1(a) and a parameterized disturbance from a magnetometer is shown in Figure 1(b).

2.4 Model Summary

Combining the batch data model with the fault model, the total model that will be studied in the sequel can be summarized as

$$\mathbb{Z} = \mathcal{O}_t x_{t-L+1} + \bar{H}_t^\theta \theta_t + \mathbb{N}_t, \tag{11}$$

where

$$\mathbb{N}_t \triangleq \bar{H}_t^v \mathbb{V} + \mathbb{E}, \tag{12}$$

and

$$S \triangleq \mathsf{Cov}(\mathbb{N}_t). \tag{13}$$

3 State Estimation

There are two unknowns in the data model (11), the initial state x_{t-L+1} and the fault profile parameter vector θ_t. This section describes different ways to estimate the initial state that are instrumental for the results in the next section. Time indices are here omitted for simplicity, e.g., $x = x_{t-L+1}$.

3.1 Least Squares Estimation

The least squares estimate of the initial state is given by

$$\hat{x} = \arg\min_x \|\mathcal{O}x - \mathbb{Z}\|_2^2, \tag{14}$$

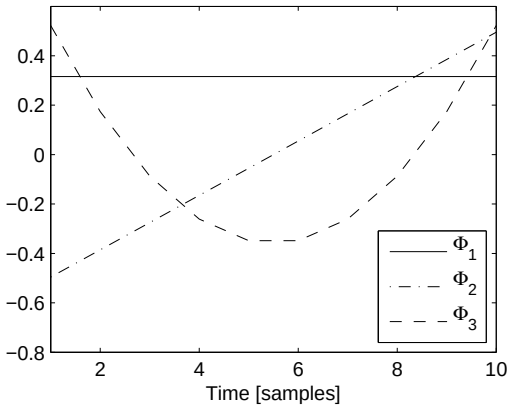

(a) Fault basis

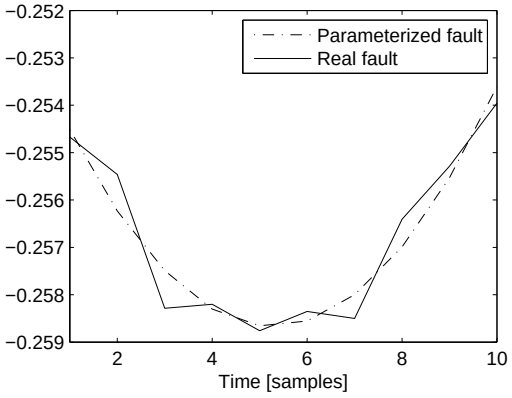

(b) Parameterized fault

Figure 1. The basis functions (a) are used to parameterize the fault from a magnetic disturbance (b).

which gives the solution

$$\hat{x} = \mathcal{O}^\dagger \mathbb{Z}. \tag{15}$$

Here, $\mathcal{O}^\dagger$ denotes the Moore-Penrose pseudo inverse of $\mathcal{O}$ (see [9]). This estimate does not account for the noise covariance S, and is included here because it is closely related to the original parity-space approach.

This estimate is unbiased in case of no fault, since

$$\mathsf{E}\,\hat{x} = \mathsf{E}\,\mathcal{O}^\dagger \mathbb{Z} = \mathsf{E}\left(x + \mathcal{O}^\dagger \mathbb{N}\right) = \mathsf{E}\,x, \tag{16}$$

and

$$\mathsf{Cov}(\hat{x}) = \mathcal{O}^\dagger S \mathcal{O}^{\dagger T}. \tag{17}$$

Observe that $\mathcal{O}^\dagger \mathcal{O} = I$ since the system is assumed to be observable and hence $\mathcal{O}$ has full column rank. In presence of faults, the expected value would be

$$\mathsf{E}\,\hat{x} = \mathsf{E}\,\mathcal{O}^\dagger \mathbb{Z} = x + \mathcal{O}^\dagger \bar{H}^\theta \theta. \tag{18}$$

3.2 Minimum Variance State Estimation

The equation system $\mathcal{O}x+\mathbb{N} = \mathbb{Z}$ is known as the *general Gauss-Markov linear model*. If $S \succ 0$, the parameters x can be estimated with minimum variance by solving the generalized least squares problem

$$\hat{x} = \arg\min_x (\mathcal{O}x - \mathbb{Z})^T S^{-1} (\mathcal{O}x - \mathbb{Z}), \tag{19}$$

see [3]. This can be rewritten as the least squares problem

$$\hat{x} = \arg\min_x \|S^{-1/2}\mathcal{O}x - S^{-1/2}\mathbb{Z}\|_2^2, \tag{20}$$

which has the solution

$$\hat{x} = (S^{-1/2}\mathcal{O})^\dagger S^{-1/2}\mathbb{Z}. \tag{21}$$

This estimate is distributed according to

$$\hat{x} \sim \mathsf{N}\left(x + (S^{-1/2}\mathcal{O})^\dagger S^{-1/2}\bar{H}^\theta\theta, (\mathcal{O}^T S^{-1}\mathcal{O})^{-1}\right). \tag{22}$$

3.3 Filtered Estimate from Past Data

Given that the data before the sliding time window are not affected by a fault (the fault detection test assumes a fault in the batch window), a suitable filter can be applied to the original model (1). For a nonlinear system a nonlinear filter, e.g., EKF, UKF, or PF, can be applied. This yields another estimate of the initial state in the batch window, independent of (21). The distribution for the initial state can then be approximated by a Gaussian distribution

$$\hat{x} \sim \mathsf{N}(x, P), \tag{23}$$

to facilitate the linear framework in the parity-space methods.

3.4 Smoothed State Estimate

Given the two estimates (22) and (23) based on independent data sets, a combined estimate can be formed similar to smoothing. Combining two independent estimates is often referred to as the *sensor fusion problem*, see for instance [10].

Denote the two distributions in (22) and (23)

$$\hat{x}^{(i)} \sim \mathsf{N}(x, P^{(i)}), \quad i = 1, 2. \tag{24}$$

Then, the smoothed initial state is estimated by

$$\hat{x} = P\Big({P^{(1)}}^{-1}\hat{x}^{(1)} + {P^{(2)}}^{-1}\hat{x}^{(2)}\Big), \tag{25}$$

where

$$P \triangleq \Big({P^{(1)}}^{-1} + {P^{(2)}}^{-1}\Big)^{-1}. \tag{26}$$

The expected value of this estimate is derived using (22) and (24)

$$\begin{aligned}\mathsf{E}\,\hat{x} &= \underbrace{P({P^{(1)}}^{-1} + {P^{(2)}}^{-1})}_{=I} x \\ &\quad + P{P^{(2)}}^{-1}(S^{-1/2}\mathcal{O})^\dagger S^{-1/2}\bar{H}^\theta\theta \\ &= x + P\mathcal{O}^T S^{-1}\bar{H}^\theta\theta \end{aligned} \tag{27}$$

Note that $\mathsf{Cov}(\hat{x}) = P \preceq P^{(2)}$ which means that the covariance of the estimate is decreased when prior information is used.

4 Fault Detection with Parity Space

The classical parity space uses a projection to construct a residual insensitive to the initial state. This section shows that this is equivalent to estimate the initial state by least squares from data in the batch and substract the estimated influence. The parity-space framework is also extended for the use of prior information about the initial state.

4.1 Classical Parity Space

The parity-space idea is to project the output on a space that is orthogonal to the influence of the initial state, the parity space. The space influenced by the initial state is spanned by $\mathcal{O}$, see (5). Thus, define $\mathcal{B}_{\mathcal{O}^\perp}$ as an orthonormal basis for $\mathcal{R}(\mathcal{O}^\perp)$. Now, a residual insensitive to the initial state can be defined as

$$r = \mathcal{B}_{\mathcal{O}^\perp}^T\,\mathbb{Z}. \tag{28}$$

The batch model (11) gives an expression for the residual suitable for analysis as

$$r = \mathcal{B}_{\mathcal{O}^\perp}^T\,\bar{H}^\theta\theta + \mathcal{B}_{\mathcal{O}^\perp}^T\,\mathbb{N} \sim \mathsf{N}(\mathcal{B}_{\mathcal{O}^\perp}^T\,\bar{H}^\theta\theta, \mathcal{B}_{\mathcal{O}^\perp}^T\,S\,\mathcal{B}_{\mathcal{O}^\perp}). \tag{29}$$

The normalized residual is then

$$\bar{r} = \underbrace{(\mathcal{B}_{\mathcal{O}^\perp}^T\,S\,\mathcal{B}_{\mathcal{O}^\perp})^{-1/2}\,\mathcal{B}_{\mathcal{O}^\perp}^T}_{\triangleq \bar{W}_1^T}\,\mathbb{Z} \sim \mathsf{N}(\bar{W}_1^T\bar{H}^\theta\theta, I). \tag{30}$$

4.2 Parity Space as Least Squares State Estimation

By inserting the least squares estimate (15) into the batch model (11), the model error is obtained as

$$\varepsilon = \mathbb{Z} - \mathcal{O}\hat{x} = \mathbb{Z} - \underbrace{\mathcal{O}\mathcal{O}^\dagger}_{\mathcal{P}_\mathcal{O}}\mathbb{Z} = (I - \mathcal{P}_\mathcal{O})\mathbb{Z} = \mathcal{P}_{\mathcal{O}^\perp}\mathbb{Z}. \tag{31}$$

Note that $\mathcal{P}_{\mathcal{O}} = \mathcal{O}\mathcal{O}^{\dagger}$ is an orthogonal projection onto the space spanned by $\mathcal{O}$ and $\mathcal{P}_{\mathcal{O}^{\perp}} = I - \mathcal{P}_{\mathcal{O}}$ is the orthogonal projection onto the complementary to $\mathcal{O}$, denoted $\mathcal{O}^{\perp}$ [16]. The projector can also be written as

$$\mathcal{P}_{\mathcal{O}^{\perp}} = \mathcal{B}_{\mathcal{O}^{\perp}} \mathcal{B}_{\mathcal{O}^{\perp}}^{T}, \tag{32}$$

where $\mathcal{B}_{\mathcal{O}^{\perp}}$ is an orthonormal basis for $\mathcal{R}(\mathcal{O}^{\perp})$.

Since the model error is computed by a rank deficient projection, the information in the prediction error can be represented by a vector of lower dimension. This low-dimensional vector is here denoted the residual. Note that $\mathcal{B}_{\mathcal{O}^{\perp}}^{T} \mathcal{B}_{\mathcal{O}^{\perp}} = I$ due to orthonormality and that the dimension is the rank of the projection in (32). The residual can be written as

$$r = \mathcal{B}_{\mathcal{O}^{\perp}}^{T} \varepsilon = \mathcal{B}_{\mathcal{O}^{\perp}}^{T} \mathcal{B}_{\mathcal{O}^{\perp}} \mathcal{B}_{\mathcal{O}^{\perp}}^{T} \mathbb{Z} = \mathcal{B}_{\mathcal{O}^{\perp}}^{T} \mathbb{Z}. \tag{33}$$

This expression equals the residual created by the classical parity-space method in Section 4.1. That is, we have shown that a hypothesis test on the model error can be reduced to a hypothesis test on the residual from the parity-space approach. Thus, these two approaches coincide.

4.3 Parity Space with Smoothing

To construct the test statistic, it is desirable to have the model error ε as a function of the measurements, $\mathbb{Z}$, and the state estimate from the previous data, $\hat{x}^{(1)}$. Thus,

$$\begin{aligned}\varepsilon &= \mathbb{Z} - \mathcal{O}\hat{x} = \mathbb{Z} - \mathcal{O}P\Big(P^{(1)^{-1}}\hat{x}^{(1)} + P^{(2)^{-1}}\hat{x}^{(2)}\Big) \\ &= \underbrace{\Big(I - \mathcal{O}PP^{(2)^{-1}}(S^{-1/2}\mathcal{O})^{\dagger}S^{-1/2}\Big)}_{\triangleq W_2^T}\mathbb{Z} - \mathcal{O}PP^{(1)^{-1}}\hat{x}^{(1)} \\ &= W_2^T\mathbb{Z} - \mathcal{O}PP^{(1)^{-1}}\hat{x}^{(1)}\end{aligned} \tag{34}$$

and the covariance is

$$\begin{aligned}\mathsf{Cov}(\varepsilon) &= W_2^T S W_2 + \mathcal{O}\underbrace{PP^{(1)^{-1}}P}_{\triangleq Q}\mathcal{O}^T \\ &= \begin{pmatrix} W_2^T & \mathcal{O} \end{pmatrix}\begin{pmatrix} S & 0 \\ 0 & Q \end{pmatrix}\begin{pmatrix} W_2 \\ \mathcal{O}^T \end{pmatrix}.\end{aligned} \tag{35}$$

It is important to note that the matrix W_2^T is time varying due to the dependence of the covariance from the filter used on data before the window. However, if a Kalman filter is used it will become stationary and then the covariance converges to a matrix which can be computed by solving the Riccati equation.

Lemma 1 *Assume that S and Q are both positive definite matrices, then the matrix in* (35) *is positive definite.*

Proof 1 *See Appendix A.*

Since $Q = PP^{(1)^{-1}}P$ where $P^{(1)}$ and P are positive definite matrices, Q is also positive definite. Then, according to Lemma 1, the covariance of ε is positive definite and thus invertible. The normalized residual can therefore be expressed as

$$\begin{aligned}\bar{r} = \mathsf{Cov}(\varepsilon)^{-1/2}\varepsilon &= \underbrace{\mathsf{Cov}(\varepsilon)^{-1/2}W_2^T}_{\triangleq \bar{W}_2^T}\mathbb{Z} \\ &\quad - \mathsf{Cov}(\varepsilon)^{-1/2}\mathcal{O}PP^{(1)^{-1}}\hat{x}^{(1)}.\end{aligned} \tag{36}$$

5 GLR Test

Detecting faults is done using the residuals derived in Section 4. Using the information about the noise distribution of the residuals, a GLR test statistic is formed. To make the decision if a fault is present or not, the test statistic is compared to a threshold from the chi-square distribution.

5.1 Test Statistic

Fault detection is here considered as detecting whether the fault is zero or not. This approach corresponds to the hypothesis test

$$\mathcal{H}_0 : \ \theta = 0 \tag{37a}$$
$$\mathcal{H}_1 : \ \theta \neq 0. \tag{37b}$$

Using the normalized residuals (30) or (36), the hypothesis test can be written as

$$\mathcal{H}_0 : \ \bar{r} \sim \mathsf{N}(0, I) \tag{38a}$$
$$\mathcal{H}_1 : \ \bar{r} \sim \mathsf{N}(\bar{W}_i^T\bar{H}^{\theta}\theta, I). \tag{38b}$$

where $i \in \{1, 2\}$ (depending on method). This yields the log-likelihood ratio

$$\begin{aligned}L &= \sup_{\theta} 2\log\left(\frac{p(\bar{r}|\,\mathcal{H}_1)}{p(\bar{r}|\,\mathcal{H}_0)}\right) \\ &= \sup_{\theta} 2\log\frac{e^{-\frac{1}{2}\|\bar{r}-\bar{W}_i^T\bar{H}^{\theta}\theta\|_2^2}}{e^{-\frac{1}{2}\|\bar{r}\|_2^2}} \\ &= \sup_{\theta} -\Big(\|\bar{r} - \bar{W}_i^T\bar{H}^{\theta}\theta\|_2^2 - \|\bar{r}\|_2^2\Big),\end{aligned} \tag{39}$$

which is maximized for $\theta = (\bar{W}_i^T\bar{H}^{\theta})^{\dagger}\bar{r}$. Then

$$\begin{aligned}L &= -\Big(\|(I - \underbrace{\bar{W}_i^T\bar{H}^{\theta}(\bar{W}_i^T\bar{H}^{\theta})^{\dagger}}_{\mathcal{P}_{\bar{W}_i^T\bar{H}^{\theta}}})\bar{r}\|_2^2 - \|\bar{r}\|_2^2\Big) \\ &= \bar{r}^T\mathcal{P}_{\bar{W}_i^T\bar{H}^{\theta}}\bar{r}\end{aligned} \tag{40}$$

5.2 Statistics

To choose suitable thresholds for the test statistics above, it is necessary to compute their distributions. While having Gaussian noise, the test statistics will be chi-square distributed variables, see [14]. The normalized residual is distributed as

$$\bar{r} \sim \mathsf{N}(\bar{W}_i^T \bar{H}^\theta \theta, I), \tag{41}$$

where $\theta = 0$ under the null hypothesis (38a). The test statistic is then distributed as the non-central chi-square distribution

$$L = \bar{r}^T \mathcal{P}_{W_i^T \bar{H}^\theta} \bar{r} \sim \chi'^2_\nu(\lambda), \tag{42}$$

where $\nu = \operatorname{rank}(W_i^T \bar{H}^\theta)$ and

$$\lambda = (W_i^T \bar{H}^\theta \theta)^T \mathcal{P}_{W_i^T \bar{H}^\theta} W_i^T \bar{H}^\theta \theta = (W_i^T \bar{H}^\theta \theta)^T W_i^T \bar{H}^\theta \theta. \tag{43}$$

Observe that $\lambda = 0$ in the fault-free case and then the test statistic is distributed according to the central chi-square distribution $L \sim \chi^2_\nu$. The threshold is then chosen from the chi-square distribution so that the fault-free hypothesis is rejected erroneously only with a small probability.

6 Application Example: Detection of Magnetic Disturbances

In many situations, the orientation of a system is of interest. To estimate the orientation, an IMU can be used. The IMU normally contains three dimensional accelerometers and gyroscopes. However, the measurements in this example are made with an IMU from Xsens Technologies, see [20], which is augmented with a magnetometer (compass) to enhance the orientation estimation. The magnetometer measures the weak magnetic field of the earth and is therefore very sensitive to disturbances from ferro-magnetic objects or electric fields. The purpose of this example is to show how these disturbances can be detected.

6.1 Modeling

To describe the behavior of the IMU, two coordinate systems are used, one fixed to the world and one fixed in the IMU (body). Denote the two coordinate systems with w and b respectively. The quaternion, q_t, is used to describe the rotation between the two coordinate systems. For a thorough review of quaternions, see [15]. The following quaternion dynamics was derived in [18]

$$q_{t+1} = \underbrace{\left(I_4 + \frac{T}{2} S(\omega^b_{bw,t})\right)}_{\triangleq F_t} q_t + \underbrace{\frac{T}{2} S'(q_t)}_{\triangleq G^v_t} v_t, \tag{44}$$

where

$$S(\omega) = \begin{pmatrix} 0 & -\omega_x & -\omega_y & -\omega_z \\ \omega_x & 0 & \omega_z & -\omega_y \\ \omega_y & -\omega_z & 0 & \omega_x \\ \omega_z & \omega_y & -\omega_x & 0 \end{pmatrix},$$

$$S'(q_t) = \begin{pmatrix} -q_1 & -q_2 & -q_3 \\ q_0 & -q_3 & q_2 \\ q_3 & q_0 & -q_1 \\ -q_2 & q_1 & q_0 \end{pmatrix}.$$

The sensors that are available in the system are gyroscopes, accelerometers and magnetometers (compass). The measurements from the gyroscopes are, as seen in (44), directly incorporated in the dynamics and are therefore not described in the measurement equations.

The accelerometers measures the earth gravitational field described in the b-system. For this example, it is assumed that the sensor is not accelerated or that the acceleration is known. The measurement equation can therefore be written as

$$y_{a,t} = g^b + e_{a,t} = \underbrace{R(q_{bw}) g^w}_{\triangleq h_a(q_{bw})} + e_{a,t}, \tag{45}$$

where the rotation matrix

$$R(q) = \begin{pmatrix} (q_0^2 + q_1^2 - q_2^2 - q_3^2) & 2(q_1 q_2 + q_0 q_3) & 2(q_1 q_3 - q_0 q_2) \\ 2(q_1 q_2 - q_0 q_3) & (q_0^2 - q_1^2 + q_2^2 - q_3^2) & 2(q_2 q_3 + q_0 q_1) \\ 2(q_1 q_3 + q_0 q_2) & 2(q_2 q_3 - q_0 q_1) & (q_0^2 - q_1^2 - q_2^2 + q_3^2) \end{pmatrix}, \tag{46}$$

g is the gravity vector and e_a is the measurement noise.

The reading from the magnetometer is a normalized vector, $\bar{n}^b_{np}$, given in the b-system and pointing along the earth magnetic field. Since the earth magnetic field is very weak, it can easily be disturbed by an electric motor or ferromagnetic objects such as beams or other iron constructions. Such a disturbance can be represented by an unknown vector, here denoted $d_{m,t}$. The measurement equation can thus be written as

$$y_{m,t} = \bar{n}^b_{np,t} + d_{m,t} + e_{m,t} = \underbrace{R(q_{bw,t}) \bar{n}^w_{np}}_{\triangleq h_m(q_{bw})} + d_{m,t} + e_{m,t}, \tag{47}$$

where $R(\star)$ is the rotation matrix given in (46), $\bar{n}_{np}$ is the normalized earth magnetic field vector and $e_{m,t}$ is the measurement noise.

The total measurement equation becomes

$$y_t = \begin{pmatrix} y_{a,t} \\ y_{m,t} \end{pmatrix} = h(q_{bw,t}) + \underbrace{\begin{pmatrix} 0 \\ I \end{pmatrix}}_{\triangleq H_{d,t}} d_{m,t} + e_t. \tag{48}$$

6.1.1 Linearization

To estimate the orientation using the EKF and to use linear theory for fault detection, the system must be linearized. The dynamic equation (44) is already linear and time-varying, but the measurement equation (48) is nonlinear. It is therefore linearized with a first order Taylor series

$$y_t = h(q_t) + e_t \approx h(\hat{q}_{t|t-1}) + H_t(q_t - \hat{q}_{t|t-1}) + H_{d,t} d_{m,t} + e_t, \tag{49}$$

where:

$$H_t = \left. \frac{\partial h(q)}{\partial q} \right|_{q=\hat{q}_{t|t-1}} \tag{50}$$

To form the linearized system, a new measurement variable is computed with known information as

$$\tilde{y}_t \triangleq y_t - h(\hat{q}_{t|t-1}) + H_t \hat{q}_{t|t-1} = H_t q_t + H_{d,t} d_{m,t} + e_t. \tag{51}$$

Then the linearized system can now be written as

$$q_{t+1} = F_t q_t + G_t^v v_t \tag{52a}$$

$$\tilde{y}_t = \underbrace{\begin{pmatrix} H_t^a \\ H_t^m \end{pmatrix}}_{=H_t} q_t + \underbrace{\begin{pmatrix} 0 \\ I \end{pmatrix}}_{=H_t^d} d_{m,t} + e_t. \tag{52b}$$

The batched form discussed in Section 2.2 will have the following form

$$\tilde{\mathbb{Y}} = \mathcal{O}_t x_{t-L+1} + \bar{H}_t^u \mathbb{U} + \bar{H}_t^d \mathbb{D} + \bar{H}_t^v \mathbb{V} + \mathbb{E}. \tag{53}$$

The linearization is done around a predicted trajectory, that is, given an estimate of the initial state in the window the trajectory is predicted in the window only using (52a).

If the fault is parameterized, it is assumed that the profile of the disturbance is a smooth function with respect to time. Thus, the disturbance could be parameterized as in Section 2.3. Each dimension in the disturbance vector is modeled separately, so $\bar{H}_t^{d^i}$ denotes the stacked system matrix for dimension i. This matrix is built up as (4) but using the i:th column of $\bar{H}_t^d$. The stacked system can now be written as

$$\tilde{\mathbb{Y}} = \mathcal{O}_t x_{t-L+1} + \sum_{i=1}^{n_d} \bar{H}_t^{d^i} \mathbb{D}^i + \bar{H}_t^v \mathbb{V} + \mathbb{E}, \tag{54}$$

where $\mathbb{D}^i = \left({d_{t-L+1}^i}^T, \ldots, {d_t^i}^T \right)^T$. Each component of the disturbance is then modeled as

$$d_t^i = \phi_{i,t}^T \theta_i. \tag{55}$$

The influence of the disturbances can now be described as

$$\begin{aligned} &\sum_{i=1}^{n_d} \bar{H}_t^{d^i} \mathbb{D}^i \\ &= \underbrace{\left(\bar{H}_t^{d^1} \cdots \bar{H}_t^{d^{n_d}} \right) \operatorname{diag}\left(\phi_{1,t}^T \cdots \phi_{n_d,t}^T \right)}_{\triangleq \bar{H}^\theta} \underbrace{\begin{pmatrix} \theta_1 \\ \vdots \\ \theta_{n_d} \end{pmatrix}}_{\triangleq \Theta}. \end{aligned} \tag{56}$$

In the tests in Section 6.3, a third order basis is chosen for the fault. A plot of the basis functions are shown in Figure 1.

6.2 Detection Algorithm

The state estimation filter, including the disturbance detection, can be described as in Algorithm 1. The fault parameterization, described above can either be used or not in step 3.

Algorithm 1. Detection Filter

(1) Time update according to an EKF.

(2) Measurement update using non-disturbed sensors. This is done according to an EKF, but the measurement equation is limited to the set of non-disturbed sensors, $\mathcal{S}$. That is

$$y = \begin{pmatrix} \vdots \\ h_i(q_t) \\ \vdots \end{pmatrix}, \quad i \in \mathcal{S}. \tag{57}$$

(3) Detection of disturbed sensors. Detection is done either according to the parity-space method or using the smoothing approach. The set $\mathcal{S}$ is updated accordingly.

6.3 Test Results

To show the performance of the disturbance detection algorithms described in previous chapter and to show the characteristics of the sensors, some measurement data is collected. The data is collected under different circumstances, i.e., when the sensor is at rest, is slowly rotated, with and without disturbances. All data is collected with a sampling rate of 100 Hz and the length of the testing window is 10 samples in all tests. Table 1 presents the datasets.

Table 1
Data sets collected using the IMU.

Data Set	Disturbance	Movement
UD1	Undisturbed	At rest
D1	Magnetometer dist	At rest
UD2	Undisturbed	Rotated around e_x^b
D2	Magnetometer dist	Rotated around e_x^b

6.3.1 Sensor at Rest

The purpose of the first data set, UD1, is to explore the noise characteristics of the sensors. The IMU is here lying still at a table and data is collected during 9 seconds. The orientation of the sensor is set so that the e_z^b-axis is pointing outwards from the earth along the gravity field (perpendicular to the table). The test statistics are shown in Figure 2. The average of the test statistic should equal the degrees of freedom in the residual, see Section 5.2. This number is plotted as a dotted line in the figure and corresponds well to the actual outcome. Note that the fault profile lowers the average of the test statistic.

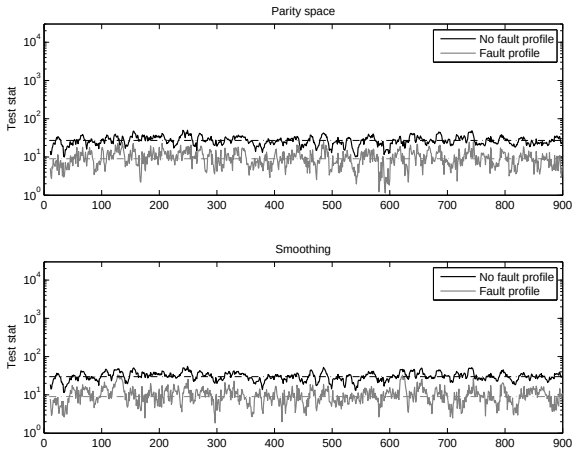

Figure 2. Test statistics for the data set UD1. Theoretical averages for undisturbed operation is plotted with dotted line.

The experiment setup for data set D1 is similar to UD1. The difference is that the magnetometer is disturbed. The disturbance was caused by a ferro-magnetic object (a pair of scissors), which was moved towards the sensor. The closest distance was approximately 30 cm. The components of the magnetometer reading are plotted in Figure 3. The test statistics are shown in Figure 4, where the disturbance is clearly detected especially when smoothing is used. Note that the average for the test statistic with fault profile is lower during the undisturbed periods, but are equal during the disturbance since the fault profile can describe this smooth type of disturbance.

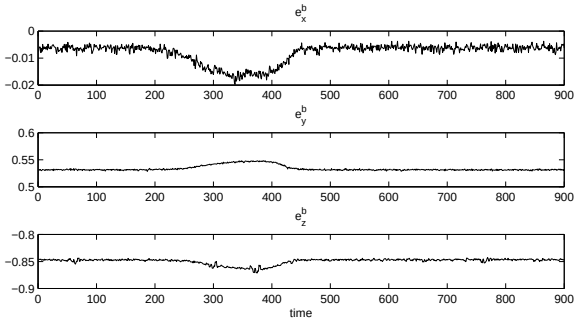

Figure 3. The components of the disturbed magnetometer readings in data set D1.

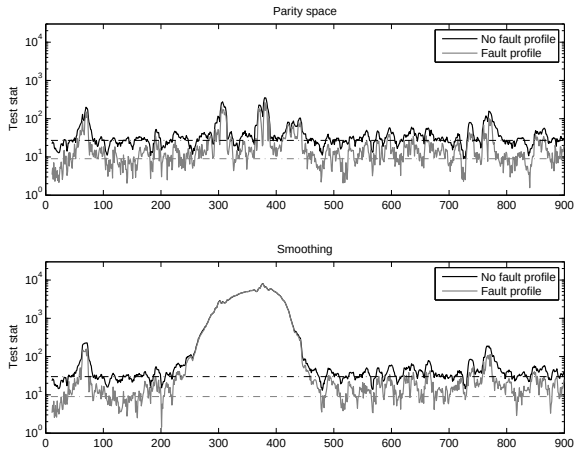

Figure 4. Test statistics for data set D1, the disturbance is clearly visible when smoothing is used. Theoretical averages for undisturbed operation is plotted with dotted line.

6.3.2 Rotating Sensor

To show the performance of detection when the sensor is rotating, data sets UD2 and D2 are collected when the IMU is rotated around the e_x^b-axis. The 3-dimensional magnetometer readings form a circle when it is not disturbed and a disturbance will make it deviate from the circle. The magnetometer readings are shown in Figure 5, where a disturbance can be seen to the right hand side in 5(b).

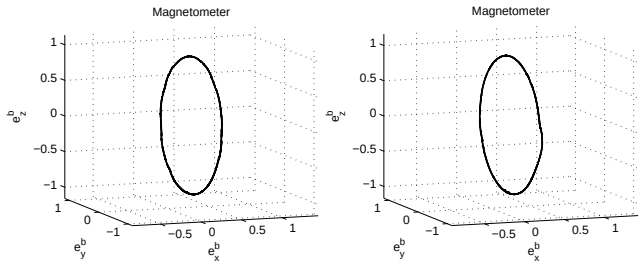

(a) Undisturbed (b) Disturbed

Figure 5. Magnetometer readings from data set UD2 (a) and D2 (b). The light disturbance for D2 is visible as a small deviation from the circle in (b).

To accurately estimate the orientation of the sensor, the accelerometer measurements has to be disregarded during acceleration of the sensor as described in Section 6.2. Even though the sensor is just rotated in this example, the accelerometer show some acceleration since they are not centered in the sensor unit. The accelerometer is therefore ignored during most of the circular movement. Figure 6 shows the test statistics for data set UD2. It can be seen here that the actual averages are a little bit higher than the theoretical average. Possible explanations are linearization errors and misalignments in the sensor configuration. The disturbance in data set D2 is clearly seen in Figure 7 both with parity space and smoothing.

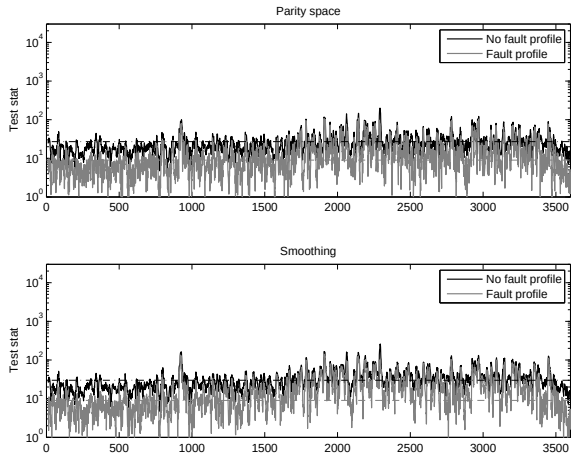

Figure 6. Test statistic for data set UD2. Theoretical averages for undisturbed operation is plotted with dotted line.

7 Conclusions and Discussion

This work started with deriving parity-space residuals using different estimates of the initial state in a batch of data. This residual and its stochastic properties were then used for creating a GLR test. This test is highly related to the GLR test in [19]. This test is defined in terms of the state space model (1) for a step fault at

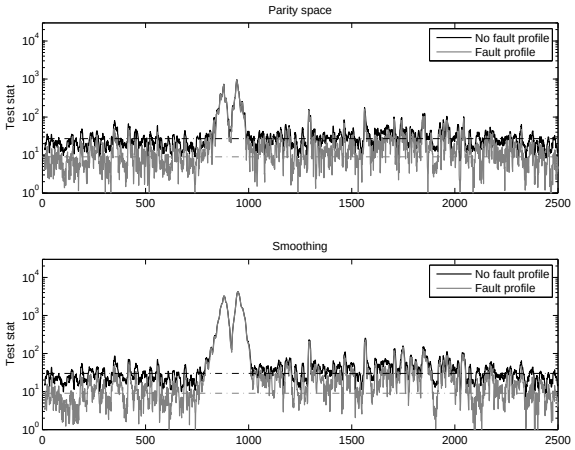

Figure 7. Test statistic for data set D2. Theoretical averages for undisturbed operation is plotted with dotted line.

an unknown time $t - L$. That is, the change time is unknown, which leads to a bank of filters, each one matched to a certain change time $t - L$. To limit computational complexity, the authors propose to only consider one fix change time $t - L$. The proposed algorithm consists of a nominal Kalman filter that runs to time t, in contrast to the Kalman filter with time lag in (23), and a matched filter that computes both an estimate of the fault and a state compensation term.

The advantage of parity space with smoothing is the geometrical interpretations and in particular its natural application to nonlinear systems. We have further pointed out how a smooth parameterization of the fault profile can improve the detection performance. Both simulations on a DC-motor and a real world example on fault detection on a magnetometer has shown to work well.

A Proof of Lemma 1

If (35) is a positive definite matrix, the following must hold

$$x^T \begin{pmatrix} W_2^T & \mathcal{O} \end{pmatrix} \begin{pmatrix} S & 0 \\ 0 & Q \end{pmatrix} \begin{pmatrix} W_2 \\ \mathcal{O}^T \end{pmatrix} x > 0 \quad \forall x \neq 0. \tag{A.1}$$

Since it is known that S and Q are positive definite, it suffices to show that

$$x^T \begin{pmatrix} W_2^T & \mathcal{O} \end{pmatrix} \neq 0 \quad \forall x \neq 0. \tag{A.2}$$

The matrix W_2^T can be written as $I - \mathcal{O}M$ where M is an arbitrary matrix. If $x \in \mathcal{N}(\mathcal{O}^T)$ and $x \neq 0$ then

$$x^T \begin{pmatrix} W_2^T & \mathcal{O} \end{pmatrix} = \begin{pmatrix} x^T & 0 \end{pmatrix} \neq 0. \tag{A.3}$$

If $x \notin \mathcal{N}(\mathcal{O}^T)$ and $x \neq 0$ then

$$x^T \begin{pmatrix} W_2^T & \mathcal{O} \end{pmatrix} = \begin{pmatrix} x^T - x^T \mathcal{O} M & x^T \mathcal{O} \end{pmatrix} \neq 0 \qquad \text{(A.4)}$$

since at least the second element is nonzero. Thus, we have shown that there is no $x \neq 0$ such that (A.2) is invalidated.

References

[1] Milton Abramowitz and Irene A. Stegun, editors. *Handbook of Mathematical Functions: with Formulas, Graphs, and Mathematical Tables*. Dover Publications, 1965.

[2] Michele Basseville and Igor V. Nikiforov. *Detection of Abrupt Changes: Theory and Application*. Information and system sciences series. Prentice Hall, Englewood Cliffs, NJ, 1993.

[3] Åke Björck. *Numerical Methods for Least Squares Problems*. SIAM Publications, 1996.

[4] A. Y. Chow and A. S. Willsky. Analytical redundancy and the design of robust failure detection systems. *IEEE Transactions on Automatic Control*, 29(7):603–614, 1984.

[5] X. Ding, L. Guo, and T. Jeinsch. A characterization of parity space and its application to robust fault detection. *IEEE Transactions on Automatic Control*, 44(2):337–343, 1999.

[6] Mitra Fouladirad and Igor Nikiforov. Optimal statistical fault detection with nuisance parameters. *Automatica*, 41:1157–1171, 2005.

[7] J. Gertler. Fault detection and isolation using parity relations. *Control Engineering Practice*, 5(5):653–661, 1997.

[8] J. J. Gertler. *Fault Detection and Diagnosis in Engineering Systems*. Marcel Dekker, Inc., 1998.

[9] Gene H. Golub and Charles F. van Loan. *Matrix Computations*. John Hopkins University Press, 3 edition, 1996.

[10] Fredrik Gustafsson. *Adaptive filtering and change detection*. John Wiley & Sons, Ltd, 2 edition, 2001.

[11] Fredrik Gustafsson. Stochastic fault diagnosability in parity spaces. In *Proceedings of the 15th IFAC World Congress*, Barcelona, Spain, July 2002.

[12] Fredrik Gustafsson. Statistical signal processing approaches to fault detection. *Annual Reviews in Control*, 31(1):41–54, 2007.

[13] Gustaf Hendeby and Fredrik Gustafsson. Detection limits for linear non-Gaussian state-space models. In *6th IFAC Symposium on Fault Detection, Supervision and Safety of Technical Processes*, Beijing, P. R. China, August–September 2006.

[14] Steven M. Kay. *Fundamentals of Statistical Signal Processing: Detection Theory*, volume 2. Prentice-Hall, Inc, 1998.

[15] Jack B. Kuipers. *Quaternions and Rotation Sequences*. Princeton Univerity Press, 1999.

[16] Carl Meyer. *Matrix Analysis and Applied Linear Algebra*. SIAM, 2000.

[17] Theodore J. Rivlin. *The Chebyshev Polynomials*. John Wiley & Sons, Inc, 1974.

[18] David Törnqvist. *Statistical Fault Detection with Applications to IMU Disturbances*. Licentiate thesis no. 1258, Department of Electrical Engineering, Linköping University, SE-581 83 Linköping, Sweden, June 2006.

[19] A.S. Willsky and H.L. Jones. A generalized likelihood ratio approach to the detection and estimation of jumps in linear systems. *IEEE Transactions on Automatic Control*, 21:108–112, 1976.

[20] Online: http://www.xsens.com, 2008.

Avdelning, Institution
Division, Department

Division of Automatic Control
Department of Electrical Engineering

Datum
Date

2008-10-03

Språk
Language

☐ Svenska/Swedish
☒ Engelska/English

☐ _____

Rapporttyp
Report category

☐ Licentiatavhandling
☐ Examensarbete
☐ C-uppsats
☐ D-uppsats
☒ Övrig rapport
☐ _____

ISBN
—

ISRN
—

Serietitel och serienummer
Title of series, numbering

ISSN
1400-3902

LiTH-ISY-R-2862

URL för elektronisk version

http://www.control.isy.liu.se

Titel
Title

Unifying the Parity-Space and GLR Approach to Fault Detection with an IMU Application

Författare
Author

David Törnqvist, Fredrik Gustafsson

Sammanfattning
Abstract

Using the parity-space approach, a residual is formed by applying a projection to a batch of observed data and this is a well established approach to fault detection. Based on a stochastic state space model, the parity-space residual can be put into a stochastic framework where conventional hypothesis tests apply. In an on-line application, the batch of data corresponds to a sliding window and in this contribution we develop an improved on-line algorithm that extends the parity-space approach by taking prior information from previous observations into account. For detection of faults, the Generalized Likelihood Ratio (GLR) test is used. This framework allows for including prior information about the initial state, yielding a test statistic with a significantly higher sensitivity to faults. Another key advantage with this approach is that it can be extended to nonlinear systems using an arbitrary nonlinear filter for state estimation, and a linearized model around a nominal state trajectory in the sliding window. We demonstrate the algorithm on data from an Inertial Measurement Unit (IMU), where small and incipient magnetic disturbances are detected using a nonlinear system model.

Nyckelord
Keywords

fault detection, parity space sensor fusion, inertial sensors, magnetometer.